Dam breach modelling: influence on downstream water levels and a proposal of a physically based module for flood propagation software

Francesco Macchione, Pierfranco Costabile, Carmelina Costanzo, Gianluca De Lorenzo and Babak Razdar

ABSTRACT

The influence exerted by the method used for computing the dam breach hydrograph on the simulated maximum water levels throughout the downstream valley is essential for selecting a specific computing module to be implemented in the numerical codes used by practitioners. This module should be able to balance the need for a reasonable physical description of the phenomenon and, at the same time, limit as much as possible the maximum number of parameters. In order to feed a debate on this field, in this paper the performances of some parametric models used for the dam breach module implemented in the popular HEC-RAS software, and a simplified but physically based model have been analysed. The performances of the dam breach models have been assessed with reference to the historical event of the Big Bay dam, using both one-dimensional and two-dimensional (1-D and 2-D) flood propagation modelling. The results show that the physically based model considered here, without any operations of ad hoc calibration, has provided the best results in predicting computation of that event. Therefore, it may be proposed as a valid alternative to parametric models, which need the estimation of some parameters that can add further uncertainties in studies like these.

Key words | 1-D and 2-D flood propagation, dam breach, environmental software, physically based model

Francesco Macchione (corresponding author)
Pierfranco Costabile
Carmelina Costanzo
Gianluca De Lorenzo
Babak Razdar
Department of Environmental and Chemical Engineering, LAMPIT (Laboratorio di Modellistica numerica per la Protezione Idraulica del Territorio),
University of Calabria,
via P. Bucci, cubo 42/B,
87036 Rende (CS),
Italy
E-mail: *francesco.macchione@unical.it*

INTRODUCTION

Flooding events are among the most catastrophic natural disasters that might provoke significant damage in properties downstream and even loss of lives. For a reliable flood risk assessment, there is a need of suitable numerical codes in order to carry out accurate computations, extended to wide areas, aimed at flood mapping and, consequently, at the implementation of defensive measures. Accurate simulations of these situations involve several key aspects ranging from the choice of the mathematical model and numerical schemes to be used in the flow propagation to the characterization of the topography and representation of the constructions that might interact with the flow patterns. In urbanized areas, it is important to describe the influence of buildings on the flow behaviour (see, for instance, Vojinovic *et al.* (2013)). More generally, it is necessary to analyse the interaction of the flow with other man-made or natural elements. Among the first ones, bridges play an important role because their piers might provoke significant backwater effects. These effects may present significant variations in water elevation on the cross section, together with a transversal regime transition within the cross section, even in straight reaches of rivers (Costabile

doi: 10.2166/hydro.2015.250

et al. 2014, 2015b). Moreover, the bridges are often obstructed by sediment or wood materials (Ruiz-Villanueva et al. 2014) and other floating materials that cannot resist the flow impacts. As regards the natural elements, often there is the need to deal with river reaches that receive significant distributed or localized lateral inflows. All the above issues require a suitable representation of the river model (Costabile & Macchione 2015; Costabile et al. 2015a). In this context, an important aspect is the availability of LIDAR (Light Detection and Ranging) data, adequately filtered, in order to automatically recognize structures that can interact with the flow propagation (Abdullah et al. 2012). However, the use of high-performance integrated hydrodynamic modelling systems seems to be necessary in order to exploit all the topographic information offered by LIDAR data (Liang & Smith 2015). For floods due to storm events, other specific issues have to be faced. In these situations, it is crucial to assess the role of the drainage system and this requires a correct evaluation of the hydraulic efficiency of the drainage network's inlets (Gómez et al. 2011; Russo et al. 2015). In all cases, it is extremely important to assess the risk to people caused by flooding (see, for instance, Russo et al. (2013)).

Further complications arise in the delimitation of flood-prone areas due to dam failures. In particular, the problem related to the computation of dam breach hydrograph shows more difficulties in cases of failures of earthfill dams, because of the physical phenomenon consisting of a progressive failure induced by the interaction between water and embankment. The prediction of these phenomena is gaining growing attention throughout the international hydraulic research community (e.g., Morris et al. 2008; Xu & Zhang 2009; Pierce et al. 2010; ASCE/EWRI 2011; Peng & Zhang 2012; Duricic et al. 2013; Wu 2013).

Several models have been proposed in the literature to simulate these kinds of situations. For example, in the last few years, rather complex models, based on shallow water equations (SWE) over a mobile bed, have been developed by Froehlich (2002), Wang & Bowles (2006), Faeh (2007) and Cao et al. (2011). Generally, these approaches include also a sudden removal of blocks or side collapses caused by undermining, and geotechnical or geometrical relationships are used for assessing the stability of breach sides. However, it is important to underline that no exhaustive theory about breach morphology and breach enlargement process, based on fluid-mechanics and soil-mechanics considerations, has been proposed yet. Moreover, they have a complex mathematical structure, describing physical processes characterized by several physical parameters, and require high computational times.

For this reason, several propagation software programs include specific modules for dam breaching based on the so-called parametric models (Wahl 1998). This is the case of widely used software such as HEC-RAS or NWS FLDWAV. In the parametric models, the hydrograph is simulated like the emptying of a reservoir through a weir in which the bottom of the breach is lowered with time and with a preset downcutting rate (Fread & Harbaugh 1973; Singh & Snorrasson 1984; Fread 1988; Walder & O'Connor 1997). Therefore, in such an approach, parameters such as the breach formation time and the final geometry of the breach have to be fixed a priori or estimated using empirical formulas. These relations are based on analyses of the data of historic events of dam failures, and estimate of breach width or failure time peak flow, as functions of representative quantities of the dam and the reservoir, such as the dam height or the water depth of the reservoir before failure, the storage volume, etc. (MacDonald & Langridge-Monopolis 1984; Froehlich 1995a, 1995b). Wahl (2004) considered several of these methods and quantified their prediction uncertainties.

One of the most important drawbacks of the parametric model is that the downcutting rate is not related to the hydraulic flow variables but, instead, is assumed a priori similarly to the failure time. Therefore, the stopping of breach developing is generally arbitrary, because it is not at all in relationship with the physical characteristics of the flow through the breach. For this reason, the use of physically based models would be better.

However, as noted above, more complicated models need several parameters and, therefore, should be used carefully only by experts. For example, in the technical manual of NWS FLDWAV (1998) it is reported: 'The BREACH model has not been directly incorporated into FLDWAV to discourage its indiscriminate use, since it should be used judiciously and with caution.'

In order to avoid the drawbacks associated with the use of more complex physically based models and the physical inconsistencies of the parametric models, a possible alternative choice is the application of simplified physically based models. In general, they take into account the eroding flow capacity (Tinney & Hsu 1961; Macchione 1986, 1989, 2008; Singh & Quiroga 1988; Singh & Scarlatos 1988; Fread 1989; Broich 2002; Hassan *et al.* 2002; Rozov 2003; Franca & Almeida 2004), which can be expressed as a function of the mean shear stress or a function of the average flow velocity on the breach.

Among the models belonging to this category, the dam-breach model proposed by Macchione (2008) predicts, in a simple but physically based manner, not only the peak discharge, but also the whole outflow hydrograph and breach development. The model considers the following issues: the geometry of the embankment, the shape of the reservoir, the shape of the breach and the hydraulic characteristics of the flow through the breach and its erosive capacity. The model needs only one calibration parameter and can be easily applied to real cases.

The non-dimensional use of the model allows one to obtain relationships for the complete discharge hydrograph fitting in case of overtopping (Macchione & Rino 2008) and for the discharge peak value fitting for both overtopping and piping cases (De Lorenzo & Macchione 2014). Excellent results have been obtained using a single value for the single calibration parameter in the simulation of 12 historic earthfill dam failures, with a discharge range covering three orders of magnitude. Moreover, the model produced very good results in the numerical simulation of experimental data (De Lorenzo & Macchione 2011).

Independently from the complexity of the mathematical model used for the generation of dam breach hydrograph, it is important to observe that the model validation is usually carried out by reproducing historical observed data of discharge peak values and typical breach features (top width, side slope and so on). All the mentioned works on the dam breach analysis focused on what has been observed at the dam site. However, a major challenge in flood mapping due to dam breaching events is understanding the influence exerted by the method used for computing the dam breach hydrograph on the flood hazard and, in particular, on the simulated maximum water levels along the valley. This paper deals with this latter issue. Therefore, this paper is based on the evaluation of dam breach models by considering the effects that the computed hydrographs induce on the maximum water levels simulated downstream, shifting the interest from the dam site to the downstream areas. This issue does not seem to be unimportant because the relevant elements for civil protection and flood risk activities are represented by the consequences induced by the flood propagation on the areas downstream, such as maximum water levels and maximum extent of flood-prone areas, flow velocity, front arrival times, etc.

In the authors' opinion, it is necessary to feed a debate on this field not only for scientific purposes but also for selecting a specific computing module, to be implemented in the technical propagation software. In particular, our intention here is to propose a method able to balance the need for a reasonable physical description of the phenomenon and, at the same time, limiting as much as possible the maximum number of parameters that the user should estimate to run the model. In particular, this last issue gained importance in the context of the reduction of the entire modelling uncertainty, ranging from the generation to the propagation of flood events.

The lack of specific studies aimed at clarifying the issues described above is somewhat expected because it is quite unusual to have well-documented historical events for both the breach generation and the water marks downstream. In particular, the breach information is quite limited to its final dimensions and, sometimes, to an estimation of the evolution time. The water surface data are almost never linked to the reservoir emptying, which can be important information for the estimation of discharge coming from the breach. Moreover, it is quite unusual to have records on the flood marks signs or other effects induced on the river bed, or on the man-made structures, downstream.

For this reason, any time it is possible to have well-documented test cases, these are extremely useful for model validation. This consideration holds for each field of water resources engineering, independently from the modelling techniques used (e.g., Chau & Wu 2010; Costabile *et al.* 2013; Taormina & Chau 2015). One of the few cases in this context is represented by the Big Bay dam, located in Lamar County, Mississippi (USA), which experienced a failure on 12 March 2004. This event has been studied by Yochum *et al.* (2008) and Altinakar *et al.* (2010) for a general reconstruction of the event.

Following the work by Yochum *et al.* (2008), this work focuses on the analysis of simplified models for dam breach simulation applied to the Big Bay dam failure, that is, to the authors' knowledge, the only case for which detailed data on flood water marks are available. The contribution of this paper is to identify a method that, on the basis of the results obtained in terms of simulated maximum water levels downstream, might effectively represent a preferential module, not only in the most common propagation software, but also for its integration in flood information systems and decision support systems (Qi & Altinakar 2011; Demir & Krajewski 2013). For the reasons explained above, this study aims to assess the performances and limits of the parametric models, widely used for technical studies, analysing their effects from the point of view of accuracy on the maximum water levels simulated downstream using two-dimensional (2-D) fully dynamic SWE. As a valid alternative to the parametric models, we propose to use the Macchione (2008) model, whose predictive ability and ease of use have already been mentioned. For the dam breaching, we have not considered more complex mathematical models because they are generally characterized by several physical parameters whose estimations introduce further uncertainties in the analysis. The propagation was preliminarily carried out with a one-dimensional (1-D) approach by means of the HEC-RAS unsteady flow option, and using as reference solution that obtained by Yochum *et al.* (2008). For the 2-D propagation, the numerical model proposed by Costabile & Macchione (2015) was used. A three-dimensional approach was not considered because the flooded areas are too large and, therefore, the computational times required for its application are not feasible for a common computing machine.

INFORMATION RELATED TO BIG BAY DAM FAILURE

The Big Bay dam breach happened in 2004, 12 years after its construction. The dam was composed of homogeneous material. It was 576 m long and 15.6 m high (excluding the foundations). Other relevant data are: longitude/latitude: 89°34′19.2″ W; 31°10′57″ N; maximum storage: 26,365,674 m^3; normal storage: 13,876,670 m^3; surface area: 3,642,171 m^2. For further information, the reader can refer to Yochum *et al.* (2008) and Altinakar *et al.* (2010).

In NWS (2004) the following news was reported: 'Beneath the dam is Bay Creek which flows into Lower Little Creek about 1 mile south of the dam. Lower Little Creek flows west into Marion county and then into the Pearl River 10 miles south of Columbia. At this time, a total of 104 homes or businesses have been damaged by the flood waters. Of the 104 damaged structures, 48 were completely destroyed, 37 sustained major damage and 19 sustained minor damage. In addition, 30 roads were damaged or closed during the event. The affected area stretched some 17 miles west of the dam to where Lower Little Creek meets the Pearl River.'

A little while after the failure, the US Geological Survey (USGS), in cooperation with the Natural Resources Conservation Service (NRCS) – US Departments of Agriculture (USDA), measured 42 high water marks (HWM) throughout the flooded areas. The HWM positions are listed in Altinakar *et al.* (2010).

The dam failure was induced by a piping phenomenon. The breach evolution is described in the event report by Burge (2004). According to the report, the embankment failed with the reservoir level at about 0.15–0.20 m above the normal pool elevation (84.73 m).

During the event, Burge recorded the breach enlargement process providing the following estimations: uncontrolled release of the lake pool began at approximately 12:25 p.m.; 12:40 p.m. breach width along crest of dam is about 75 feet in width; 12:50 p.m. breach widened to about 150 feet; 1:10 p.m. breach widens to ±200 feet; 1:40 p.m. breach about 350 feet wide. Moreover, Burge reports that 'at 2:25 p.m. flow continuing to slow, flood pool dropping rapidly, scour hole becoming visible' and 'at 2:40 p.m. water surface at about 240 elevation, flow very stable'. For this reason, it seems that the most significant part of the flow hydrograph was developed between 12:25 and 2:40 p.m., so that the duration is 2 hr and 15 min.

The final breach geometry, estimated by Yochum *et al.* (2008) considering the summer 2004 aerial photography, highlighted a bottom width equal to 70 m and the top width equal to 96.0 m. Therefore, the side slope (horizontal/vertical) was 0.61 on the right side and 1.3 on the left. The breach finally reached the original ground elevation (71.3 m).

COMPUTATION OF DAM BREACH HYDROGRAPH

The Macchione (2008) model

In this work, the Macchione (2008) model has been used for the numerical simulation of the dam-breaching hydrograph. The governing equations of the model can be found in Macchione (2008) and Macchione & Rino (2008). The range 0.05–0.10 m/s can be used for the calibration parameter v_e. In particular, the mean value 0.07 m/s should be used when cases of dams similar to those examined in Macchione (2008) have to be simulated.

The numerical simulation of the event has been carried out using the available observed data concerning, essentially, the observed breach, the total volume that came out from the breach and the reservoir emptying time. This observation has been described in the previous section and is reported in Table 1.

As noted by Macchione (2008), the representative parameter of the total eroded volume is the mean breach width and not the top one. For this reason, information about the temporal enlargement of top width is not so important, because the temporal evolution of the breach shape is unknown. Therefore, the attention here is devoted to the final mean width of the breach reported by Yochum et al. (2008).

Using the data related to the observed breach, three discharge hydrographs have been obtained using the Macchione model. Since the dam failure was induced by erosion at the base of the embankment, an initial triangular breach with height equal to dam height has been assumed for all the simulations.

The Macchione (2008) model has been used here both in a 'predictive' and a 'calibrated' way. As already noted, the Macchione model has only one parameter v_e, for which the author, in his original paper, has suggested a specific value ($v_e = 0.07$ m/s) and, furthermore, the side slope value $\tan\beta$ is assumed equal to 0.2.

Therefore, the first configuration considered in the paper, and hereafter named M1, refers to the Macchione model used in its predictive mode, that is, $v_e = 0.07$ m/s and $\tan\beta = 0.2$. The temporal evolution of the mean breach width (b_{average}) is shown in Figure 1. Moreover, since we are considering a well-documented dam breach event, it is particularly interesting to compute also the hydrographs that can be obtained removing the assumption related to side slope in the predictive version of the Macchione model, setting its value equal to the mean value observed for the aerial picture, that is, 0.995, keeping $v_e = 0.07$ m/s. This configuration will be identified as M2 (see Figure 2). Finally, in order to explore all the possible situations, we have assumed again $\tan\beta = 0.2$ but we have considered the parameter v_e as a calibration parameter, setting it to $v_e = 0.09$ m/s, that is, that value for which the simulated mean value of the final breach is equal to that estimated from the aerial photography. This is the hydrograph M3. The results are shown in Figure 3.

Since M2 and M3 are based on observed data, they can be considered as two historical reconstructions of the event. M1 instead represents the results of the Macchione model used in a predictive mode, since it is based on the standard value suggested by Macchione (2008) for the parameter v_e. The most important results of the hydrographs are summarized in Table 2.

HEC-RAS dam breach computation

Besides the hydrographs computed using the Macchione (2008) model, in this paper the hydrographs computed by

Table 1 | Observed data: breach information, discharged volume, reservoir emptying time

	Time	12:25	12:40	12:50	1:10 pm	1:40 pm
Breach data from Burge (2004)	Breach width	Breach initial formation	75 m	150 m	200 m	350 m
Summer 2004 aerial photography	Breach bottom width	70 m				
	Top width	96 m				
	Average width	83 m				
	Horizontal/vertical side slopes	0.61 (right hand) and 1.3 (left hand)				
Hydrograph	Volume	17,500,000 m^3				
	Duration	2.25 hours				

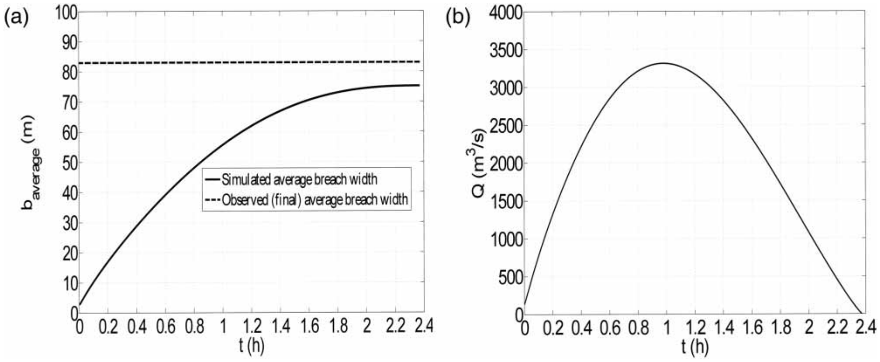

Figure 1 | Simulation of the temporal behaviour of both the mean breach width and the hydrograph using the Macchione (2008) model: v_e=0.07 m/s and tanβ = 0.2 (M1 hydrograph).

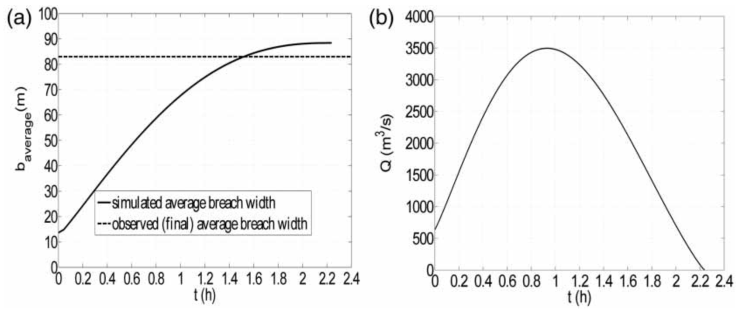

Figure 2 | Simulation of the temporal behaviour of both the mean breach width and the hydrograph using the Macchione (2008) model: v_e = 0.07 m/s and tanβ = 0.955 (M2 hydrograph).

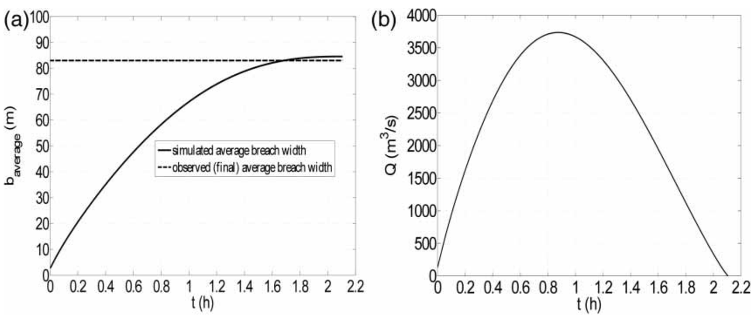

Figure 3 | Simulation of the temporal behaviour of both the mean breach width and the hydrograph using the Macchione (2008) model: v_e = 0.09 m/s and tanβ = 0.2 (M3 hydrograph).

Yochum *et al.* (2008), using the dam breach option within HEC-RAS, have been considered. The following information is taken from Yochum *et al.* (2008): 'The breach hydrograph was created with breach geometry measured primarily from aerial photography and breach formation time developed from Burge (2004). Breach progression was assumed to follow a sine wave. The breach formation time is estimated to be 55 min. Volume of the HEC-RAS developed breach hydrograph was 17,500,000 m^3, matching the estimated storage available at the time of failure with an initial water surface elevation of 84.89 m.'

The hydrograph used by Yochum *et al.* (2008) will be named HR. The authors computed also another two hydrographs, which will be referred to here as FR and ML. They

Table 2 | Simulated results obtained by the different versions of the Macchione (2008) model

Hydrograph's ID	v_e (m/s)	tanβ	Simulated average breach width (m)	Error (%)	Duration of the simulated hydrograph (h)	Peak discharge (m^3/s)
M1	0.07	0.2	75	−10	2.4	3,313
M2	0.07	0.955	88	+6	2.2	3,497
M3	0.09	0.2	85	+2	2.1	3,733

were obtained using the parameters provided using the formulas proposed by Froehlich (1995a, 1995b) and MacDonald & Langridge-Monopolis (1984), respectively.

The main characteristics of the hydrographs are summarized in Table 3.

1-D FLOOD PROPAGATION

An accurate 1-D numerical simulation of flood propagation was obtained by Yochum *et al.* (2008) using the hydrograph HR obtained with the dam breach module implemented in the well-known HEC-RAS software. This module is based on the parametric approach for the dam breach modelling. This requires, as input, the values of the final breach width and its developing time.

In order to compare all the simulations, methods for measuring quantitative performance should be used (Bennett *et al.* 2013). In particular, we have considered the mean error, the mean absolute error and their standard deviation (SD) that, in the classification provided by Bennett *et al.* (2013) have been considered as 'direct value comparison' whose purpose is to test whether the model output shows similar characteristics as a whole to the set of the comparison data.

Considering the actual dam breach geometry, and inserting the Manning coefficient values estimated by visual inspection, Yochum *et al.* (2008) calculated water-surface elevations with an absolute average error of 0.34 m, with respect to measured HWM.

Using the same geometry and roughness coefficients considered by Yochum *et al.* (2008), we have obtained the results summarized in Table 4 while, in Table 5, the associated performances ranking is reported.

Discussion on the 1-D simulation

Nowadays, the use of 1-D modelling might appear as an obsolete approach, since the increasing understanding of the hydraulic phenomena, the developing of more and more robust and reliable numerical models, the increasing availability of high-resolution topographic data and the advance in computing technology allow scientists and engineers to use 2-D or even, for limited areas, three-dimensional (3-D) models. Despite the limitations of 1-D

Table 3 | Information related to the numerical hydrographs used in the computations

Model	Hydrograph's ID	Assumed values for the parameters: v_e (m/s)	Breach side slopes	Average breach width (m)	Breach formation time (h)	Peak discharge (m^3/s)
Macchione (2008)	M1	0.07	0.2	–	–	3,313
	M2	0.07	0.955	–	–	3,497
	M3	0.09	0.2	–	–	3,733
HEC-RAS + observed parameters	HR	–	1.3 & 0.6 (observed)	83.2 (observed)	0.92 (observed)	4,160
HEC-RAS + Froehlich (1995a, 1995b) parameters	FR	–	0.9	61.5	1.7	2,700
HEC-RAS + MacDonald & Langridge-Monopolis (1984) parameters	ML	–	0.5	59.6	1.0	3,130

Table 4 | 1-D flood propagation result

					HR*			M1			M2			M3			FR			ML		
River Sta	**Distance (km)**	**Observed W.M.E. (m a.s.l.)**	**Water marks ID**	**Min Ch El (m)**	***Q* (m^3/s)**	**W.S.E. (m a. s.l.)**	**Error (m)**	***Q* (m^3/s)**	**W.S.E. (m a. s.l.)**	**Error**	***Q* (m^3/s)**	**W.S.E. (m a. s.l.)**	**Error (m)**	***Q* (m^3/s)**	**W.S.E. (m a. s.l.)**	**Error (m)**	***Q* (m^3/s)**	**W.S.E. (m a. s.l.)**	**Error (m)**	***Q* (m^3/s)**	**W.S.E. (m a. s.l.)**	**Error (m)**
496048*	1.148	75.07	21	67.97	4,030	75.08	0.01	3,279	74.64	−0.43	3,457	74.75	−0.32	3,692	74.89	−0.18	2,761	74.29	−0.78	3,079	74.5	−0.57
495418	1.313	74.92	17	67.12	4,020	74.33	−0.59	3,277	73.97	−0.95	3,454	74.07	−0.85	3,689	74.18	−0.74	2,759	73.67	−1.25	3,075	73.85	−1.07
494416*	1.616	73.49	20	66.14	3,940	72.91	−0.58	3,253	72.57	−0.92	3,429	72.66	−0.83	3,657	72.78	−0.71	2,735	72.21	−1.28	3,035	72.42	−1.07
493621*	1.858	73.03	18	65.94	3,930	72.43	−0.6	3,240	72.12	−0.91	3,415	72.21	−0.82	3,641	72.33	−0.7	2,727	71.82	−1.21	3,023	71.97	−1.06
489003	3.266	69.19	23–25	60.84	3,020	69.81	0.62	2,869	69.74	0.55	3,002	69.85	0.66	3,151	69.96	0.77	2,395	69.31	0.12	2,473	69.37	0.18
480714	5.792	66.45	27	57.18	2,290	66.52	0.07	2,291	66.52	0.07	2,370	66.61	0.16	2,456	66.71	0.26	2,004	66.19	−0.26	2,021	66.22	−0.23
480601	5.826	65.86	26&29	57.18	2,550	65.54	−0.32	2,620	65.62	−0.24	2,732	65.7	−0.16	2,845	65.77	−0.09	2,145	65.24	−0.62	2,178	65.27	−0.59
474299	7.747	63.09	19	55.47	2,100	63.46	0.37	2,332	63.61	0.52	2,424	63.66	0.57	2,479	63.69	0.6	1,854	63.27	0.18	1,871	63.28	0.19
471891	8.480	62.36	16	53.34	1,970	62.34	−0.02	2,186	62.56	0.2	2,259	62.62	0.26	2,305	62.65	0.29	1,764	62.17	−0.19	1,778	62.18	−0.18
461552	11.627	59.04	41	49.77	1,470	59.12	0.08	1,712	59.28	0.24	1,771	59.33	0.29	1,773	59.32	0.28	1,398	58.98	−0.06	1,404	58.99	−0.05
450426	15.018	55.66	40	46.79	1,150	54.76	−0.9	1,302	55.03	−0.63	1,336	55.09	−0.57	1,324	55.06	−0.6	1,135	54.74	−0.92	1,137	54.74	−0.92
435769	19.486	50.81	39	41.76	978	50.93	0.12	1,109	51.14	0.33	1,139	51.18	0.37	1,123	51.16	0.35	978	50.93	0.12	979	50.93	0.12
408806	27.703	43.1	32&33	35.05	797	42.95	−0.15	883	43.16	0.06	910	43.21	0.11	889	43.17	0.07	803	42.97	−0.13	803	42.97	−0.13
406278	28.474	42.39	34&37	34.35	784	42.05	−0.34	868	42.29	−0.1	891	42.35	−0.04	874	42.3	−0.09	790	42.07	−0.32	791	42.07	−0.32
406278	28.474	42.43	38	34.35	784	42.05	−0.38	868	42.29	−0.14	891	42.35	−0.08	874	42.3	−0.13	791	42.07	−0.36	791	42.07	−0.36
406117	28.523	42.09	35&36	34.35	781	41.76	−0.33	865	41.91	−0.18	888	41.95	−0.14	870	41.92	−0.17	788	41.77	−0.32	788	41.77	−0.32
398757	30.766	38.92	9	33.38	770	39.32	0.4	843	39.45	0.53	865	39.48	0.56	848	39.46	0.54	769	39.33	0.41	769	39.33	0.41
398594	30.812	38.8	7	33.38	762	39.07	0.27	846	39.19	0.39	865	39.22	0.42	848	39.19	0.39	769	39.08	0.28	769	39.08	0.28

*Results by Yochum *et al.* (2008).

Table 5 | Performances of the numerical hydrographs sorted by absolute error

	Absolute error (m)		Error (m)	
Simulation 1-D	Mean	SD	Mean	SD
HR	0.34	0.25	−0.13	0.41
M3	0.39	0.25	0.01	0.47
M2	0.40	0.27	−0.02	0.49
M1	0.41	0.29	−0.09	0.51
ML	0.45	0.35	−0.32	0.48
FR	0.49	0.42	−0.37	0.53

modelling, highlighted by the 2-D approach in flood mapping using LIDAR-DEM (Costabile *et al.* 2015a), in the case of rivers with both low sinuosities and not too wide floodplains, the 1-D approach is sufficient for solving certain types of flooding problems (Macchione & Viggiani 2004). Moreover, 1-D modelling still remains a preferential approach considering the limited data requirement in respect of 2-D or 3-D models and it is very efficient from a computational point of view, especially for operations carried out in real time. Furthermore, 1-D performances can be improved adding terms representing the momentum exchange between the main channel and the floodplain in order to describe the flow dynamics in rivers with wide floodplains better (Cao *et al.* 2006; Huthoff *et al.* 2008; Proust *et al.* 2009; Costabile & Macchione 2012). For these reasons, it is particularly interesting to analyse the performances obtained in the simulations of flood propagation of the dam breach hydrograph using 1-D modelling.

The errors reported in Table 4 can be considered very low, considering the fact that floods due to dam failure are characterized by very high water depths. For the HR hydrograph the error ranges between −0.90 m and +0.62 m; for the M1 hydrograph between −0.95 and +0.55; for the M2 hydrograph between −0.85 m and +0.66 m; for the M3 hydrograph between −0.74 m and +0.77 m; for the FR hydrograph between −1.28 m and +0.41 m; for the ML hydrograph between −1.07 m and +0.41 m. The mean error values are also very low. Among all the computed hydrographs, the M3 hydrograph gives the closest value of the mean error to zero, followed by the M2, M1 and HR ones. The FR and ML hydrographs show a tendency to underestimate the maximum water surface elevations. In terms of absolute error, the best results have been achieved by the HR hydrograph (0.34 m), followed by M3 (0.39 m), M2 (0.40 m), M1 (0.41 m), ML (0.45 m) and FR (0.49 m). The hydrograph obtained using the three versions of the Macchione (2008) model gave very similar results.

In order to evaluate the accuracy of the results throughout the downstream valley, the errors have been computed subdividing the domain into two parts. In particular, the HWM data set has been split into two parts, dividing by two the total number of HWM, so that we separated the points belonging to the upstream and downstream areas of the domain. The results are reported in Tables 6 and 7. Upstream, the best result has been provided by the HR hydrograph, in terms of absolute error, and by the M3 in terms of mean error. Therefore, the analysis of HWM upstream confirmed the ranking of the total data set discussed above. Downstream, the best results have been obtained using M2, M1 and M3, followed

Table 6 | 1-D simulation results for the upstream 50% of water elevations

	Upstream HWM (21, 17, 20, 18, 23–25, 27, 26–29,19, 16)			
	Error (m)		Absolute error (m)	
Simulation 1-D	Mean	SD	Mean	SD
HR	−0.116	0.440	0.353	0.262
M3	−0.056	0.577	0.482	0.272
M2	−0.148	0.599	0.514	0.292
M1	−0.234	0.606	0.532	0.333
ML	−0.489	0.511	0.571	0.404
FR	−0.588	0.581	0.654	0.494

Table 7 | 1-D simulation results for the downstream 50% of water elevations

	Downstream HWM (41, 40, 39, 32–33, 34–37, 38, 35–36, 9, 7)			
	Error (m)		Absolute error (m)	
Simulation 1-D	Mean	SD	Mean	SD
M2	0.102	0.350	0.287	0.205
M1	0.056	0.360	0.289	0.197
M3	0.071	0.357	0.291	0.194
ML	−0.143	0.399	0.323	0.255
FR	−0.144	0.399	0.324	0.254
HR	−0.137	0.401	0.330	0.244

by ML, FR and HR. All the hydrographs gave very similar results downstream.

Discussion on the bridge effects

As is well known, bridges might influence the water surface profile in a river during a flood event. In fact, the presence of bridges, with piers in the river bed, represents an alteration of the natural geometry of the river cross section because they can induce significant obstacles to the river flow. The effects on the flow dynamics can be considerable. In particular, a major effect consists in an increase of water surface elevation upstream of the bridge structure (backwater effect), above the normal water surface profile that would occur without the bridge. Moreover, it has been recently observed that they can induce 2-D effects even in a straight reach along which the suitability of 1-D approaches is generally accepted (Costabile *et al.* 2014, 2015b). In this study, the bridge effects have been analysed using the same HEC-RAS project, but removing the bridges previously considered (see Table 8). This evaluation has been carried out using only the HR hydrograph. The results obtained with bridges are very similar to those computed by Yochum *et al.* (2008). The absolute error, equal to 0.33 m in the simulation with bridges (HR), becomes 0.38 m removing the bridges (HR-WB). The mean error is −0.098 m for HR and −0.212 for HR-WB. The maximum difference in the computation of water surface elevations between HR and HR-WB is −0.81 m and it is located just upstream of the Roadway Bridge (River Station 480714).

All in all, according to HEC-RAS computation, it seems that the bridges had a limited influence on the flood flow, probably due to the limited narrowing induced by piers located in the riverbed. In fact, the ratio between the total width of the piers and transversal length of the bridge ranges from 2% (Chaney Church Roadway Bridge) to 7% (Columbia-Purvis Roadway Bridge).

2-D FLOOD PROPAGATION

A first study related to the 2-D flood propagation was presented by Altinakar *et al.* (2010), who used the SWE solved using a first order finite-volume upwind method. They used a structured mesh and the element side was equal to 20 m. The computational domain was obtained starting from a 10 m digital elevation model (DEM), available at Mississippi Automated Resource Information System (MARIS). A constant value (0.05 $m^{-1/3}s$) throughout the domain was used for the Manning coefficient. The authors did not consider the bridges in their simulation. The hydrograph flowing through the breach was computed using the same final breach geometry assumed by Yochum *et al.* (2008). In order to obtain the same discharge peak as Yochum *et al.* (2008), by a trial and error procedure they assumed the breaching duration equal to 38 min, obtaining a discharge peak value equal to 4,155 m^3/s.

On the basis of the authors' experience in the performance of flood propagation models (Costabile *et al.* 2012), in this paper, the 2-D simulation has been performed using a numerical code based on the fully dynamic SWE applied to a computational domain composed of an unstructured grid with irregular triangular elements. This choice is motivated by the fact that it allows one to modify the density of the grid points accordingly to the topographic features and the expected hydraulic situations. Its high degree of flexibility provides an accurate geometrical description of the river reach, even in the presence of significant topographical gradients or when the hydraulic variables are expected to change very rapidly (hydraulic jump, shock wave and so on). For this reason, we have preferred to use an unstructured grid instead of a structured one.

The mathematical model is based on the 2-D SWE that can be expressed in the following form:

$$\frac{\partial \mathbf{U}}{\partial t} + \frac{\partial \mathbf{F}}{\partial x} + \frac{\partial \mathbf{G}}{\partial y} = \mathbf{S} \tag{1}$$

where:

$$\mathbf{U} = \begin{pmatrix} h \\ hu \\ hv \end{pmatrix}; \tag{2}$$

$$\mathbf{F} = \begin{pmatrix} hu \\ hu^2 + gh^2/2 \\ huv \end{pmatrix}; \tag{3}$$

Table 8 | 1-D simulation results with and without bridges

River Sta	Observed W.M.E. (m a.s.l.)	Water Marks ID	Min Ch El (m a.s.l.)	Simulation with bridges Q (m^3/s)	W.S.E. (m a.s.l.)	Error 1 (m)	Simulation without bridges Q (m^3/s)	W.S.E. (m a.s.l.)	Error 2 (m)	Error 2 -Error 1 (m)
496048	75.07	21	67.97	4080	75.11	0.04	4080	74.93	−0.14	−0.18
495418	74.92	17	67.12	4071	74.36	−0.56	4059	74.01	−0.91	−0.35
495360	Columbia-Purvis Roadway Bridge									
494416	73.49	20	66.14	4000	72.93	−0.56	3999	72.93	−0.56	0
493621	73.03	18	65.94	3983	72.45	−0.58	398	72.45	−0.58	0
489003	69.19	23-25	60.84	3061	69.84	0.65	3047	69.81	0.62	−0.03
488950	Salt Dome Roadway Bridge									
480714	66.45	27	57.18	2312	66.55	0.1	2539	65.74	−0.71	−0.81
480665	Chaney Church Roadway Bridge									
480601	65.86	26&29	57.18	2589	65.58	−0.28	2530	65.55	−0.31	−0.03
474299	63.09	19	55.47	2158	63.49	0.4	2194	63.08	−0.01	0.39
471950	Luther Saucier Roadway Bridge									
471891	62.36	16	53.34	2016	62.38	0.02	2036	62.42	0.06	0.04
461620	Pinebur Roadway Bridge (upper)									
461552	59.04	41	49.77	1511	59.08	0.04	1611	59.18	0.14	0.1
450426	55.66	40	46.79	1174	54.8	−0.86	1238	54.91	−0.75	0.11
435769	50.81	39	41.76	1001	50.97	0.16	1038	50.88	0.07	−0.09
435695	Pinebur Roadway Bridge (lower)									
408806	43.1	32&33	35.05	812	42.99	−0.11	837	42.97	−0.13	−0.02
406278	42.39	34&37	34.35	799	42.09	−0.3	821	41.93	−0.46	−0.16
406278	42.43	38	34.35	799	42.09	−0.34	821	41.93	−0.5	−0.16
406200	MS-13 Roadway Bridge									
406117	42.09	35&36	34.35	796	41.79	−0.3	819	41.83	−0.26	−0.04
398757	38.92	9	33.38	776	39.34	0.42	796	39.21	0.29	−0.13
398675	MS-43 Roadway Bridge									
398594	38.8	7	33.38	776	39.09	0.29	796	39.12	0.32	0.03
Mean error						**−0.098**			**−0.21**	
Mean absolute error						**0.33**			**0.38**	
Standard deviation (error)						**0.41**			**0.42**	
Standard deviation (absolute error)						**0.24**			**0.27**	

$$\mathbf{G} = \begin{pmatrix} hv \\ huv \\ hv^2 + gh^2/2 \end{pmatrix}; \tag{4}$$

$$\mathbf{S} = \begin{pmatrix} q \\ gh\left(S_{0x} - S_{fx}\right) \\ gh\left(S_{0y} - S_{fy}\right) \end{pmatrix} \tag{5}$$

in which: t is time; x, y are the horizontal coordinates; h is the water depth; u, v are the depth-averaged flow velocities in x- and y-directions, respectively; g is the gravitational acceleration; S_{0x}, S_{0y} are the bed slopes in x- and y-directions; S_{fx}, S_{fy} are the friction slopes in x- and y-directions computed using the Manning formula; q is a lateral inflow.

For the numerical integration of system (1), in this paper the finite volume methodology has been used. We have used this methodology because it is a well-consolidated approach in flood propagation studies (for a general review, see for example Toro & García-Navarro (2007)). All the details about the numerical flux (Roe's scheme) and source terms computations, wet-dry treatment and grid generation process can be found in Costabile & Macchione (2015) and are not reported here for the sake of brevity.

The analysis discussed here is based on a 10 m DEM, available at the National Map Viewer provided by USGS (United States Geological Service). The elevation data, composing the National Elevation Dataset, have been published using different spatial resolutions. The studied area is covered only in part by the 3 m DEM and, for this reason, the analysis presented here has been carried out using only the 10 m DEM. In particular, the data refer to a survey performed in 1999 and are available in NAD1983 reference system.

The upstream boundary condition is represented by the hydrographs synthetically reported in Table 2. The downstream boundary condition has been set according to the flow regime: transmissive boundary condition for supercritical flow and critical flow for subcritical condition. In reality, the boundary cells are located very far (>2 km) from the last water marks and, consequently, the effects of the physical condition imposed there have no particular influences on the results.

As already performed by Altinakar *et al.* (2010), the simulation has been carried out without inserting the bridges.

Discussion on the 2-D simulation

Currently it seems that numerical modelling of flood wave propagation based on SWE is shifting from 1-D to 2-D models. In the last years, the increasing use of 2-D models over 1-D has been partly fueled by developments in DEM, especially from airborne LIDAR data. Furthermore, recent studies highlighted conceptual problems with the 1-D approach applied to overbank flows when compared to the flow behaviour simulated by the 2-D models (see for example Tayefi *et al.* (2007) and Costabile *et al.* (2015a)).

The analysis of the area downstream the Big Bay dam shows a braided development of the river reach and for this reason one of the hypotheses at the basis of 1-D modelling, that is horizontal water surface and uniform velocity across the section, is somewhat questionable. For this reason, in order to reduce the uncertainty related to the description of the flow behaviour, the application of the 2-D modelling seems to be essential for the scope of this paper.

The numerical results obtained using 2-D modelling are summarized in Table 9. First of all, it should be observed that some HWM elevations are lower than the bed elevations (see HWM number 33, 34, 10 and 11). This fact might be induced by an uncertainty in the high marks measurements or in the DEM used.

Neglecting those water marks for which the simulations have predicted a dry bed, the errors range from −1.6 m to +0.8 m. The performances of each simulation are summarized in Table 10. All the simulations are characterized by a negative mean error. The lowest error is equal to 0.34 m, provided by the simulation with the M3 hydrograph. The highest error is equal to −0.48 m, obtained by the simulation with the FR hydrograph. The presented ranking has been organized according to the mean error values and it is the same as the absolute error. The lowest errors have been achieved by using the M3 hydrograph, calibrated in order to have the simulated final mean breach equal to the observed one. The simulation based on the M2 hydrograph, calibrated in order to have the same mean side slope of the breach, is in second position while the M1 hydrograph, that is the Macchione (2008) model with the standard value of the parameters, is in third position. The list ends with the HR, ML and FR hydrographs.

The negative sign of the mean error highlights that all the simulations have underestimated the observed values. This effect might be induced by the roughness coefficient assumed in the computations and, for this reason, another run of the HR hydrograph has been performed. In particular, the roughness value has been set to 0.07 $m^{-1/3}s$ from 0.05 $m^{-1/3}s$. The results, reported in Table 11, show that the increase in the roughness values only lead to a slight reduction of the mean error and the SD.

Moreover, the effect of the bridges that have not been considered in the above-presented computations should be checked. The bridge influence has been taken into account only by the insertion of the bridge abutments, because the obstruction induced by piers is very limited. The results

Table 9 | 2-D simulation results

			M1		M2		M3		HR		ML		FR	
Water marks no.	Observed W.S.E. (m a.s.l)	Bed elevation	W.S.E. (m a.s.l)	Error (m)	W.S.E. (m a.s.l)	Error (m)	W.S.E. (m a.s.l)	Error (m)	W.S.E. (m a.s.l)	Error (m)	W.S.E. (m a.s.l)	Error (m)	W.S.E. (m a.s.l)	Error (m)
21	75.07	74.38	74.38	−0.69	74.38	−0.69	74.39	−0.68	74.40	−0.67	74.38	−0.69	74.38	−0.69
17	74.92	73.20	73.30	−1.62	73.33	−1.59	73.38	−1.54	73.47	−1.45	73.27	−1.65	73.24	−1.68
22	72.33	70.71	70.73	−1.60	70.77	−1.56	70.79	−1.54	70.79	−1.54	70.71	−1.62	70.71	−1.62
20	73.49	72.42	72.52	−0.97	72.57	−0.92	72.62	−0.87	72.73	−0.76	72.49	−1.00	72.46	−1.03
18	73.03	71.95	72.02	−1.01	72.04	−0.99	72.09	−0.94	72.19	−0.84	72.00	−1.03	71.98	−1.06
23	69.19	68.28	68.45	−0.74	68.49	−0.70	68.53	−0.66	68.49	−0.70	68.37	−0.83	68.36	−0.83
28	65.75	63.72	65.06	−0.69	65.12	−0.63	65.19	−0.56	65.05	−0.70	64.78	−0.97	64.79	−0.96
29	65.75	63.59	65.03	−0.72	65.09	−0.66	65.16	−0.59	65.02	−0.73	64.73	−1.02	64.73	−1.02
27	66.45	64.55	65.30	−1.15	65.34	−1.11	65.38	−1.07	65.30	−1.15	65.12	−1.33	65.12	−1.33
26	65.96	65.33	65.48	−0.48	65.51	−0.45	65.54	−0.42	65.48	−0.48	65.40	−0.56	65.40	−0.56
16	62.36	60.56	62.17	−0.19	62.20	−0.16	62.23	−0.13	62.08	−0.28	61.93	−0.43	61.94	−0.42
41	59.07	57.09	58.81	−0.26	58.83	−0.24	58.84	−0.23	58.67	−0.40	58.59	−0.48	58.60	−0.47
42	59.13	58.43	59.11	−0.02	59.14	0.01	59.16	0.03	58.99	−0.14	58.93	−0.20	58.93	−0.20
40	55.66	55.00	55.57	−0.09	55.58	−0.08	55.60	−0.06	55.41	−0.25	55.35	−0.31	55.36	−0.30
39	50.81	47.02	50.69	−0.12	50.69	−0.12	50.71	−0.11	50.50	−0.31	50.48	−0.33	50.48	−0.33
33	43.07	43.95	43.95	0.88	43.95	0.88	43.95	0.88	43.95	0.88	43.95	0.88	43.95	0.88
32	43.13	42.79	42.87	−0.26	42.87	−0.26	42.87	−0.26	42.83	−0.30	42.83	−0.30	42.83	−0.30
37	42.49	40.02	42.10	−0.39	42.11	−0.38	42.12	−0.37	41.88	−0.61	41.88	−0.61	41.88	−0.61
38	42.43	41.68	42.04	−0.39	42.05	−0.38	42.05	−0.38	41.91	−0.52	41.91	−0.52	41.91	−0.52
36	42.06	40.18	41.45	−0.61	41.46	−0.60	41.47	−0.59	41.27	−0.79	41.26	−0.80	41.26	−0.80
35	42.12	41.28	41.74	−0.38	41.74	−0.38	41.75	−0.37	41.65	−0.47	41.64	−0.48	41.65	−0.47
34	42.28	42.44	42.44	0.16	42.44	0.16	42.44	0.16	42.44	0.16	42.44	0.16	42.44	0.16
10	38.62	38.81	39.10	0.48	39.10	0.48	39.11	0.49	39.02	0.40	39.01	0.39	39.01	0.39
9	38.92	36.92	38.28	−0.65	38.28	−0.64	38.28	−0.64	38.20	−0.72	38.20	−0.72	38.20	−0.72
11	38.47	39.31	39.32	0.85	39.32	0.85	39.32	0.85	39.31	0.84	39.31	0.84	39.31	0.84
8	38.68	36.69	38.23	−0.45	38.23	−0.45	38.24	−0.44	38.16	−0.52	38.16	−0.52	38.16	−0.52
14	38.89	36.79	38.78	−0.11	38.78	−0.11	38.79	−0.10	38.69	−0.20	38.69	−0.20	38.69	−0.20
13	38.89	36.29	38.75	−0.14	38.75	−0.14	38.75	−0.14	38.66	−0.23	38.66	−0.23	38.66	−0.23
7	38.8	34.69	38.66	−0.14	38.66	−0.14	38.67	−0.13	38.57	−0.23	38.57	−0.23	38.57	−0.23
6	38.77	36.33	38.61	−0.16	38.61	−0.16	38.61	−0.16	38.52	−0.25	38.52	−0.25	38.52	−0.25
4	38.74	37.29	38.51	−0.23	38.51	−0.23	38.51	−0.23	38.42	−0.32	38.42	−0.32	38.42	−0.32
5	38.74	37.75	38.55	−0.19	38.55	−0.19	38.56	−0.18	38.47	−0.27	38.47	−0.27	38.47	−0.27
3	38.71	37.76	38.44	−0.27	38.44	−0.27	38.45	−0.26	38.37	−0.34	38.36	−0.35	38.37	−0.34
1	38.71	37.63	38.42	−0.29	38.42	−0.29	38.43	−0.28	38.34	−0.37	38.34	−0.37	38.34	−0.37
2	38.74	37.70	38.43	−0.31	38.43	−0.31	38.43	−0.31	38.35	−0.39	38.35	−0.39	38.35	−0.39

Table 10 | Statistics related to the 2-D propagation of the flood hydrographs (simulation without bridges)

	Absolute error (m)		Error (m)	
2-D simulation without bridges	**Mean**	**SD**	**Mean**	**SD**
M3	0.476	0.385	−0.338	0.514
M2	0.492	0.396	−0.356	0.525
M1	0.505	0.405	−0.370	0.535
HR	0.548	0.342	−0.418	0.496
ML	0.608	0.391	−0.478	0.546
FR	0.609	0.396	−0.480	0.550

Table 11 | Influence of the roughness values on the 2-D propagation results (HR hydrograph)

	Absolute error (m)		Error (m)	
2-D simulation without bridges	**Mean**	**SD**	**Mean**	**SD**
HR, $n = 0.05\ \mathrm{m}^{-1/3}\mathrm{s}$	0.54	0.36	−0.41	0.50
HR, $n = 0.07\ \mathrm{m}^{-1/3}\mathrm{s}$	0.49	0.27	−0.37	0.43

are summarized in Table 12. The mean error is lower than the simulation with bridges, but just by a few centimetres, confirming the fact that bridges' narrowing influence is very low. The absolute error is practically the same as before. Moreover, the ranking of the results related to the hydrographs used still holds. Once again, the lowest errors have been obtained using the M3 hydrographs.

In conclusion, the 2-D computations have highlighted absolute errors between 0.5 and 0.6 m and mean errors ranging from −0.5 m to −0.3 m. They are comparable to those obtained by Altinakar *et al.* (2010) using a 20 m DEM. The mean error values have been slightly influenced by inserting the bridge abutments or by increasing the roughness and, therefore, we can conclude that the roughness values' estimations are good enough for this case and that the bridges have not influenced significantly the simulation.

For the event considered here, it seems that the sources of uncertainties are mainly limited to the topographic data or to phenomena not explicitly considered here like debris transport or morphological bed variations. Anyway, the results can be considered satisfactory in terms of prediction of the event.

Finally, in order to evaluate the trend of the performances throughout the valley, the errors have been computed separating the upstream points from the downstream ones. The results are presented in Tables 13 and 14. For both the data sets, the best result has been achieved

Table 12 | Statistics related to the 2-D propagation of the flood hydrographs (simulation with bridges)

	Absolute error (m)		Error (m)	
2-D simulation with bridges	**Mean**	**SD**	**Mean**	**SD**
M3	0.47	0.39	−0.27	0.54
M2	0.49	0.39	−0.29	0.56
M1	0.51	0.40	−0.31	0.57
HR	0.53	0.33	−0.34	0.53
ML	0.61	0.39	−0.42	0.59
FR	0.61	0.40	−0.45	0.60

Table 13 | 2-D simulation results for the upstream 50% of water elevations

Upstream HWM (21, 17, 22, 20, 18, 23–25, 28, 29, 27, 26, 16, 41, 42, 40, 39, 33, 32)	Error (m)		Absolute error (m)	
	Media	**SD**	**Media**	**SD**
M3	−0.515	0.597	0.622	0.477
M2	−0.546	0.608	0.651	0.487
M1	−0.572	0.618	0.676	0.494
HR ($n = 0.05$)	−0.577	0.553	0.681	0.408
ML	−0.698	0.606	0.801	0.449
FR	−0.701	0.613	0.805	0.457

Table 14 | 2-D simulation results for the downstream 50% of water elevations

Downstream HWM (37, 38, 36, 35, 34, 10, 9, 11, 8, 14, 13, 7, 6, 4, 5, 3, 1)	Error (m)		Absolute error (m)	
	Media	**SD**	**Media**	**SD**
M3	−0.172	0.363	0.338	0.204
M2	−0.177	0.364	0.342	0.204
M1	−0.178	0.364	0.343	0.204
HR ($n = 0.05$)	−0.268	0.395	0.422	0.207
FR	−0.270	0.396	0.425	0.207
ML	−0.270	0.396	0.425	0.207

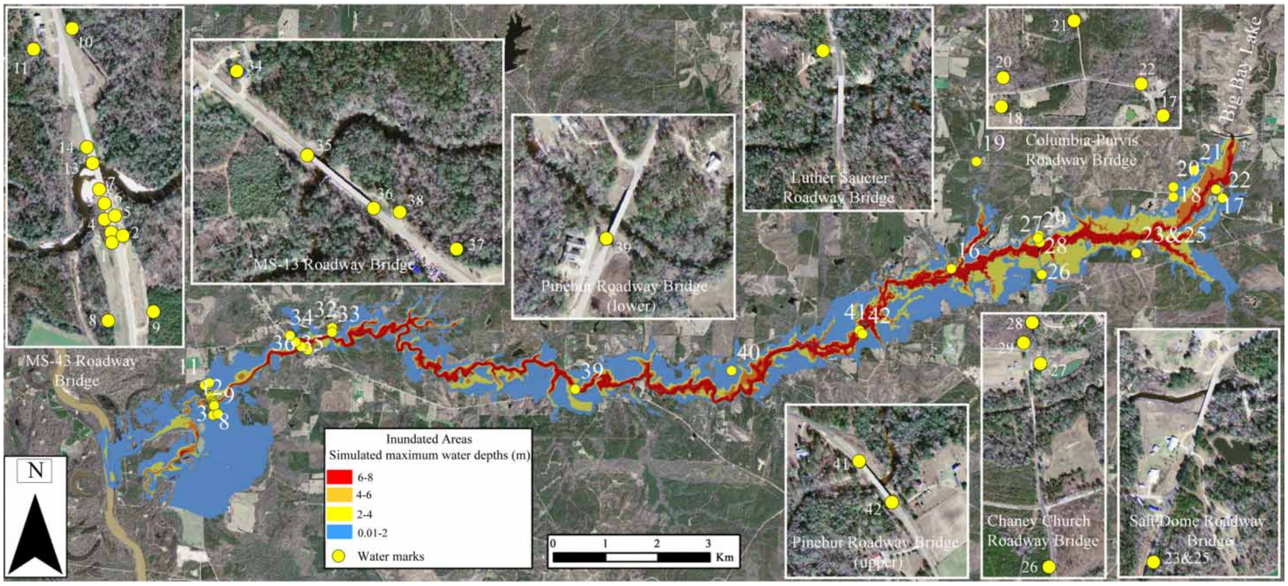

Figure 4 | Maximum water depths simulated using the Macchione (2008) model (M1 hydrograph, 2-D simulation).

by the M3 hydrograph, followed by M2, M1, HR, ML and FR. Therefore, the ranking discussed above has been confirmed also by this kind of analysis.

The maximum water levels simulated by the 2-D model based on the M1 hydrograph are shown in Figure 4 while, in Figure 5, the evolution of flood propagation is depicted.

CONCLUSION

The aim of this paper is to provide a contribution for selecting the most suitable dam breach model to be used in flood mapping studies and, consequently, to be implemented in common flood propagation software. For this reason, the analysis has been carried out focusing on the water levels of the flow propagating downstream.

To achieve this purpose, following the work by Yochum *et al.* (2008), in this paper the Big Bay dam failure has been considered, for which not only observed breach data but also HWM throughout the valley are available. The little influence that the bridges seem to have exerted on the flood makes this case study useful for comparing the effects on the propagation due to the different boundary conditions, represented by the breach hydrographs.

As done by Yochum *et al.* (2008), we have considered the so-called parametric models, which are, nowadays, the ones most used in commercial software. Moreover, they are easier to use than more complex models based on geotechnical or geometrical relationships for assessing the stability of breach sides, which demonstrate an important drawback for technical studies since they have many parameters whose estimation increases the global uncertainty of the entire modelling chain (generation and propagation of the hydrograph).

To overcome the drawbacks arising from the use of the above parametric approaches, the use of the Macchione (2008) model has been proposed for its remarkable predictive ability and its ease of use.

Regarding the flood propagation modelling, this research has been carried out using HEC-RAS as a 1-D approach and a finite volume method based on an unstructured grid recently proposed by Costabile & Macchione (2015) for the 2-D analysis.

Six hydrographs have been considered in this work. The first three have been simulated using HEC-RAS and the same river model considered by Yochum *et al.* (2008) in order to make the comparison easier. For the breach parameters, the authors used observed data (the HR hydrograph), and those obtained using the formulas

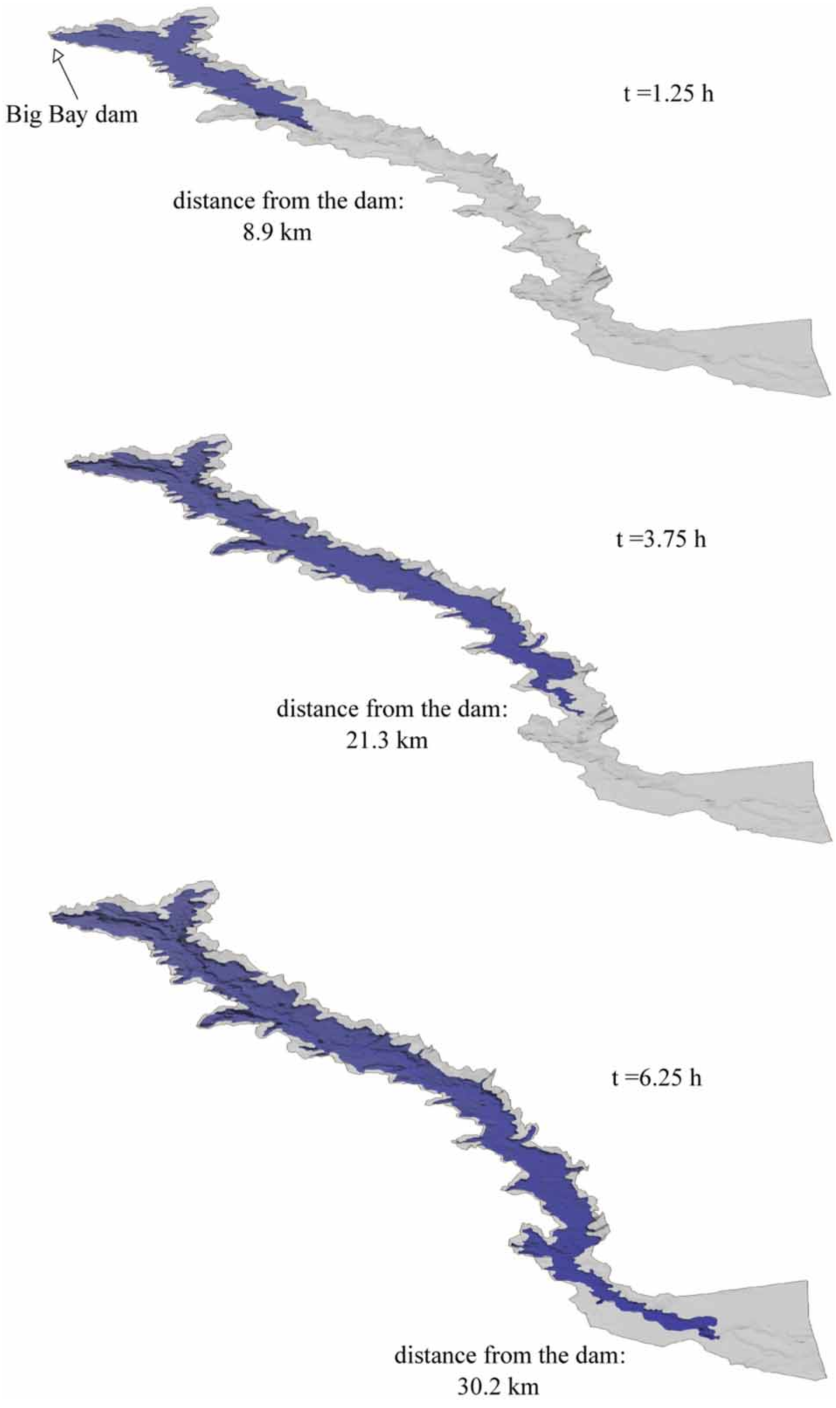

Figure 5 | Flood propagation evolution simulated using the Macchione (2008) model (M1 hydrograph).

proposed by Froehlich (1995a, 1995b) (the FR hydrograph) and MacDonald & Langridge-Monopolis (1984) (the ML hydrograph). The Macchione (2008) model has been used in three different ways: the first one is based on the values of the parameters proposed by the author in his original work, so that the model is intended to work in a predictive mode. In the other two options, one parameter has been set ad hoc.

The comparison between the simulated maximum water levels and the observed HWM shows a substantial similitude among the results obtained using the different hydrographs.

Despite the uncertainties due to the topography used for the generation of the DEM, the absolute errors in terms of simulated maximum water levels, obtained using all the hydrographs, are quite limited if compared with the high water depths that characterize the event.

For the 1-D calculations, the lowest absolute error has been obtained using the HR hydrograph, while the lowest mean value has been obtained using the M3 hydrograph. However, it should be observed that the HR hydrograph has been computed inserting the historical observed data and the M3 has been obtained by setting ad hoc one parameter of the Macchione (2008) model in order to have the final mean breach width equal to the observed one.

For predictive purposes, Yochum *et al.* (2008) have estimated some breach parameters using the Froehlich (1995a, 1995b) and MacDonald & Langridge-Monopolis (1984) formulas. This approach gave less accurate results than those obtained using the M1 hydrograph, i.e., the Macchione (2008) model used in a predictive mode.

It may be important to underline that the hydrographs have shown different peak values. For example, the use of HR and M3 hydrographs has provided similar results in terms of simulated water levels, but they are characterized by different values of peak discharge, 4,160 m^3/s and 3,733 m^3/s, respectively. It is interesting to note that although the HR hydrograph simulated a higher peak value than the M3 hydrograph (a difference up to 427 m^3/s), the latter seems to provide less underestimation of the maximum water levels than the HR hydrograph.

As for the 2-D modelling results, the best numerical *reconstruction* of the event has been provided by the M3 hydrograph while the most accurate *prediction* has been obtained by the M1 hydrograph. The simulation results based on the M1 hydrograph have been even better than those obtained using the HR hydrograph, despite the fact that, as already mentioned, historical data have been inserted as input for the computation of the HR hydrograph.

For this reason, the results presented here allow one to underline an important conclusion. In its predictive mode (the M1 hydrograph), that means no calibration parameter has to be tuned because the suggested values are used, the Macchione (2008) model has provided reliable and similar, at least or even better, results to those that can be simulated using the parametric models, which need the estimation of some parameters that can add further uncertainties in studies like these.

Therefore, the analysis carried out in this work suggests that the Macchione (2008) model, whose numerical code written in Matlab is reported in the Appendix (available with the online version of this paper), can be effectively nested in the flood propagation software, to support or substitute those currently used, for three reasons at least: its predictive ability, the absence of calibration parameter to be set ad hoc and the ease of use.

The conclusions of this work are relevant and provide an important contribution to practical guidance on flood hazard resulting from dam breaches but are somewhat limited by the single case that is available in the literature. Moreover, it would have been interesting to extend this analysis in a situation for which the flow produces significant morphological variations to the river bed. From this point of view, further developments of this work are necessarily linked to the availability of well-documented test cases.

ACKNOWLEDGEMENTS

The authors want to thank Steven E. Yochum for sharing the topographic and computations data related to his study.

REFERENCES

Abdullah, A. F., Vojinovic, Z., Price, R. K. & Aziz, N. A. A. 2012 Improved methodology for processing raw LIDAR data to support urban flood modelling – accounting for elevated roads and bridges. *J. Hydroinform.* **14** (2), 253–269.

Altinakar, M. S., McGrath, M. Z., Ramalingam, V. P. & Omari, H. 2010 2D modelling of Big Bay Dam failure in Mississippi: Comparison with field data and 1D model results. River Flow 2010. *Proceedings of International Conference on Fluvial Hydraulics*, 8–10 September, Braunschweig, Germany (A. Dittrich, K. Koll, J. Aberle & P. Geisenhainer, eds), Vol. 1, Bundesanstalt fur Wasserbau (BAW), Karlsruhe, Germany, pp. 547–554.

ASCE/EWRI 2011 Earthen embankment breaching. *J. Hydraul. Eng.* **137** (12), 1549–1564.

Bennett, N. D., Croke, B. F. W., Guariso, G., Guillaume, J. H. A., Hamilton, S. H., Jakeman, A. J., Marsili-Libelli, S., Newham, L. T. H., Norton, J. P., Perrin, C., Pierce, S. A., Robson, B., Seppelt, R., Voinov, A. A., Fath, B. D. & Andreassian, V. 2013 Characterising performance of environmental models. *Environ. Modell. & Softw.* **40**, 1–20.

Broich, K. 2002 Description of the parameter model DEICH-P. Tech. Report, University of the Federal Armed Forces Munich. http://www.impact-project.net/wp2_technical.htm.

Burge, T. R. 2004 *Big Bay Dam: Evaluation of Failure.* Land Partners Limited Partnership, Hattiesburg, MS.

Cao, Z., Meng, J., Pender, G. & Wallis, S. 2006 Flow resistance and momentum flux in compound open channel. *J. Hydraul. Eng.* **132** (12), 1272–1282.

Cao, Z. X., Yue, Z. Y. & Pender, G. 2011 Landslide dam failure and flood hydraulics. Part II: coupled mathematical modelling. *Nat. Hazard.* **59** (2), 1021–1045.

Chau, K. W. & Wu, C. L. 2010 A hybrid model coupled with singular spectrum analysis for daily rainfall prediction. *J. Hydroinform.* **12** (4), 458–473.

Costabile, P. & Macchione, F. 2012 Analysis of one-dimensional modeling for flood routing in compound channels. *Water Resour. Manage.* **26**, 1065–1087.

Costabile, P. & Macchione, F. 2015 Enhancing river model set-up for 2-D dynamic flood modeling. *Environ. Modell. Softw.* **67**, 89–107.

Costabile, P., Costanzo, C. & Macchione, F. 2012 Comparative analysis of overland flow models using finite volume schemes. *J. Hydroinform.* **14** (1), 122–135.

Costabile, P., Costanzo, C. & Macchione, F. 2013 A storm event watershed model for surface runoff based on 2D fully dynamic wave equations. *Hydrol. Process.* **27**, 554–569.

Costabile, P., Macchione, F., Natale, L. & Petaccia, G. 2014 Representing skewed bridge crossing on 1-D and 2-D flood propagation models: compared analysis in practical studies. In: *Proceedings of the International Conference on Fluvial Hydraulics, River Flow 2014* (A. J. Schleiss, G. De Cesare, M. J. Franca & M. Pfister, eds), CRC Press/Balkema, Leiden, The Netherlands, pp. 733–741.

Costabile, P., Macchione, F., Natale, L. & Petaccia, G. 2015a Flood mapping using LIDAR DEM. Limitations of the 1-D modeling highlighted by the 2-D approach. *Nat. Hazard.* **77**, 181–204.

Costabile, P., Macchione, F., Natale, L. & Petaccia, G. 2015b Comparison of scenarios with and without bridges and analysis of backwater effect in 1-D and 2-D river flood modeling. *Comput. Modell. Eng. Sci.* **109** (2), 81–103.

De Lorenzo, G. & Macchione, F. 2011 Capability of a numerical model to simulate dam breach laboratory tests. *J. Flood Risk Manage.* **4**, 298–305.

De Lorenzo, G. & Macchione, F. 2014 Formulas for the peak discharge from breached earthfill dams. *J. Hydraul. Eng.* **140** (1), 56–67.

Demir, I. & Krajewski, W. F. 2013 Towards an integrated flood information system: centralized data access, analysis, and visualization. *Environ. Modell. Softw.* **50**, 77–84.

Duricic, J., Erdik, T. & van Gelder, P. 2013 Predicting peak discharge due to embankment dam failure. *J. Hydroinform.* **15** (4), 1361–1376.

Faeh, R. 2007 Numerical modelling of breach erosion of river embankments. *J. Hydraul. Eng.* **133** (9), 1000–1009.

Franca, M. J. & Almeida, A. B. 2004 A computational model of rockfill dam breaching caused by overtopping (RoDaB). *J. Hydraul. Res.* **42** (2), 197–206.

Fread, D. L. 1988 *BREACH: An Erosion Model for Earthen Dam Failures*. Report, US National Weather Service, Silver Spring, MD (revised 1991).

Fread, D. L. 1989 National weather service models to forecast dam breach floods. In: *Hydrology of Disasters* (O. Starosolszky & O. Melder, eds), James and James, London, pp. 192–211.

Fread, D. L. & Harbaugh, T. E. 1973 Transient hydraulic simulation of breached earth dams. *J. Hydraul. Div.* **99** (1), 139–154.

Froehlich, D. C. 1995a Embankment dam breach parameters revisited. In: *Proceedings of the 1995 ASCE Conference on Water Resources Engineering*, San Antonio, Texas, pp. 887–891 (August).

Froehlich, D. C. 1995b Peak outflow from breached embankment dams. *J. Water Resour. Plann. Manage.* **121** (1), 90–97.

Froehlich, D. C. 2002 Impact project field tests 1 and 2: "blind" simulation by davef. In: *Proceedings of 2nd IMPACT Project Workshop*, 12–13 September, Mo-i-Rana, Norway.

Gómez, M., Macchione, F. & Russo, B. 2011 Methodologies to study the surface hydraulic behavior of urban catchments during storm events. *Water Sci. Technol.* **63** (11), 2666–2673.

Hassan, M. A. A. M., Samuels, P., Morris, M. & Gathaora, D. 2002 Improving the accuracy of predictions of breach formation through embankment dams and flood embankments. In: *River Flow 2002, Proceedings of the International Conference on Fluvial Hydraulics* (D. Bousmar & Y. Zech, eds), Vol. 1, Balkema, Liss, The Netherlands.

Huthoff, F., Roos, P. C., Augustijn, D. C. M. & Hulscher, S. 2008 Interacting divided channel method for compound channel flow. *J. Hydraul. Eng.* **134** (8), 1158–1165.

Liang, Q. & Smith, L. S. 2015 A high-performance integrated hydrodynamic modelling system for urban flood simulations. *J. Hydroinform.* **17** (4), 518–533.

Macchione, F. 1986 Sull'idrogramma di piena conseguente alla rottura degli sbarramenti in materiali sciolti [Outflow hydrograph due to earthfill dam breaching]. *Memoria Interna no. 139*, Dipartimento di Difesa del Suolo, Università della Calabria, Cosenza (in Italian).

Macchione, F. 1989 Discussion on: dimensionless analytical solution for dam breach erosion. *J. Hydraul. Res.* **27** (2), 447–452.

Macchione, F. 2008 Model for predicting floods due to earthen dam breaching. I: formulation and evaluation. *J. Hydraul. Eng.* **134** (12), 1688–1696.

Macchione, F. & Rino, A. 2008 Model for predicting floods due to earthen dam breaching. II: comparison with other methods and predictive use. *J. Hydraul. Eng.* **134** (12), 1697–1707.

Macchione, F. & Viggiani, G. 2004 Simple modelling of dam failure in a natural river. *Water Manage.* **157**, 53–60.

MacDonald, T. C. & Langridge-Monopolis, J. 1984 Breaching characteristics of dam failures. *J. Hydraul. Eng.* **110** (5), 567–586.

Morris, M. W., Hanson, G. J. & Hassan, M. 2008 Improving the accuracy of dam breach modelling: why are not we progressing faster? *J. Flood Risk Manage.* **1**, 150–161.

NWS 2004 Big Bay Lake Dam Break. National Weather Service Forecast Office, Online report. http://www.srh.noaa.gov/jan/?n=2004_03_12_big_bay_lake_dam_break.

NWS FLDWAV 1998 NWS FLDWAV model: Theoretical description by D. L. Fread; User documentation by J. M. Lewis. November 28, 1998. Hydrologic Research Laboratory – Office of Hydrology – National Weather Service (NWS), NOAA, Silver Spring, MD. http://www.rivermechanics.net/models/fldwav_doc.pdf.

Peng, M. & Zhang, L. M. 2012 Breaching parameters of landslide dams. *Landslides* **9** (1), 13–31.

Pierce, M. W., Thornton, C. I. & Abt, S. R. 2010 Predicting breach outflow from breached embankment dams. *J. Hydrol. Eng.* **15** (5), 338–349.

Proust, S., Bousmar, D., Riviere, N. & Paquier, Z. Y. 2009 Nonuniform flow in compound channel: a 1-D method for assessing water level and discharge distribution. *Water Resour. Res.* **45**, W12411.

Qi, H. & Altinakar, M. S. 2011 A GIS-based decision support system for integrated flood management under uncertainty with two dimensional numerical simulations. *Environ. Modell. Softw.* **26**, 817–821.

Rozov, A. L. 2003 Modeling of washout of dams. *J. Hydraul. Res.* **41** (6), 565–577.

Ruiz-Villanueva, V., Bladé, E., Sánchez-Juny, M., Marti-Cardona, B., Díez-Herrero, A. & Bodoque, J. M. 2014 Two-dimensional numerical modeling of wood transport. *J. Hydroinform.* **16** (5), 1077–1096.

Russo, B., Gómez, M. & Macchione, F. 2013 Pedestrian hazard criteria for flooded urban areas. *Nat. Hazard.* **69**, 251–265.

Russo, B., Sunyer, D., Velasco, M. & Djordjević, S. 2015 Analysis of extreme flooding events through a calibrated 1D/2D coupled model: the case of Barcelona (Spain). *J. Hydroinform.* **17** (3), 473–491.

Singh, K. P. & Snorrasson, A. 1984 Sensitivity of outflow peaks and flood stages to the selection of dam breach parameters and simulation models. *J. Hydrol.* **68**, 295–310.

Singh, V. P. & Quiroga, C. A. 1988 Dimensionless analytical solution for dam breach erosion. *J. Hydraul. Res.* **26** (2), 179–197.

Singh, V. P. & Scarlatos, P. D. 1988 Analysis of gradual earth dam failure. *J. Hydraul. Eng.* **114** (2), 21–42.

Taormina, R. & Chau, K. W. 2015 Neural network river forecasting with multi-objective fully informed particle swarm optimization. *J. Hydroinform.* **17** (1), 99–113.

Tayefi, V., Lane, S. N., Hardy, R. J. & Yu, D. 2007 A comparison of one- and two-dimensional approaches to modelling flood inundation over complex upland floodplains. *Hydrol. Proces.* **21**, 3190–3202.

Tinney, E. R. & Hsu, Y. H. 1961 Mechanics of washout of an erodible fuse plug. *J. Hydraul. Div.* **87**, 1–29.

Toro, E. F. & García-Navarro, P. 2007 Godunov-type methods for free-surface shallow flows: a review. *J. Hydraul. Res.* **45** (6), 736–751.

Vojinovic, Z., Seyoum, S., Salum, M. H., Price, R. K., Fikri, A. K. & Abebe, Y. 2013 Modelling floods in urban areas and representation of buildings with a method based on adjusted conveyance and storage characteristics. *J. Hydroinform.* **15** (4), 1150–1168.

Wahl, T. L. 1998 *Prediction of Embankment Dam Breach Parameters – A Literature Review and Needs Assessment*. Report DSO-98-004, US Department of Interior – Bureau of Reclamation, Denver, CO.

Wahl, T. L. 2004 Uncertainty of prediction of embankment dam breach parameters. *J. Hydraul. Eng.* **130** (5), 389–397.

Walder, J. S. & O'Connor, J. E. 1997 Methods for predicting peak discharge of floods caused by failure of natural and constructed earthen dams. *Water Resour. Res.* **33** (10), 2337–2348.

Wang, Z. & Bowles, D. 2006 Three-dimensional non-cohesive earthen dam breach model. Part 1: theory and methodology. *Adv. Water Resour.* **29**, 1528–1545.

Wu, W. 2013 Simplified physically based model of earthen embankment breaching. *J. Hydraul. Eng.* **139** (8), 837–851.

Xu, Y. & Zhang, M. 2009 Breaching parameters for earthfill and rockfill dams. *J. Geotech. Geoenviron. Eng.* **135** (12), 1957–1970.

Yochum, S. E., Goertz, L. A. & Jones, P. H. 2008 Case study of the Big Bay dam failure: accuracy and comparison of breach predictions. *J. Hydraul. Eng.* **134** (9), 1285–1293.

First received 13 July 2015; accepted in revised form 7 November 2015. Available online 19 December 2015